Co-Design of Wireless Sensor-Actuator Networks for Building Controls

Alie El-Din Mady and Gregory Provan

Abstract— A Building Automation System (BAS) aims to provide good user comfort within occupied zones in a building. One can enhance the functionality of a BAS through embedding advanced control strategies within a Wireless Sensor/Actuator Network (WSAN), and also make retrofit applications possible. However, control systems that are embedded in a WSAN can perform sub-optimally if the control system and WSAN are designed independently. In this context, we develop a co-design approach for embedding BAS code within a Network Control System. We compare our developed system for building lighting control with (a) a standard PI control method to empirically demonstrate a 19% reduction in energy use and 65% improvement in user comfort, and (b) an MPC strategy that uses only presence-based control, to show 25% reduction in energy use. Our approach also improves network delay and sensor battery usage by 68% over the PI baseline.

I. INTRODUCTION

The household and industrial building sector consumes around 40% of total energy use in the West, and accounts for nearly one-third of greenhouse gas emissions. Of this figure, approximately one-third can be attributed to the lighting systems present in buildings [1]. There is now a significant effort being devoted to reducing these energy costs.

Many buildings incorporate a Building Management System (BMS) to maintain a comfortable environment in an energy-efficient manner. A typical BMS provides a core functionality that keeps the building's climate within a specified range, automates the lighting and Heating, Ventilation and Air-Conditioning (HVAC) based on building schedules, and monitors system performance and device failures.

In this article, we focus on advanced lighting control systems, which aim to minimize energy use while maintaining comfortable indoor light levels by adapting to variations in external light while minimizing glare from windows. Glare can be a particular problem in offices, as it can hamper the use of computer monitors. More recent approaches for reducing energy use in advanced lighting systems have included presence-based lighting, which activates indoor lights only when rooms are occupied, and automated blinds, which optimize indoor light levels, minimize glare and control indoor temperatures. To introduce such new higher-performance lighting systems in legacy systems, it is typically cheaper to embed the new sensor/control systems within a Wireless Sensor/Actuator Network (WSAN) rather than rewire legacy systems. In this article, we assume that we will embed an advanced lighting system within a WSAN. Such a WSAN-based control architecture is called a Networked Control System (NCS).

We examine the hardware/software co-design of a wireless WSAN for building actuation control applications, in which we aim to minimize user discomfort and energy usage. To study the tradeoffs in the design process, we define our objective function as consisting of two parts: (a) a Quality of Service (QoS) function for the WSAN, defined as a joint function of network delay and sensor battery usage; and (b) a Quality of Control (QoC) function for the control application running on the WSAN, defined as a joint function of user discomfort and HVAC energy usage.

We empirically show how reduced QoS results in decreased QoC. Given this relationship, the optimization function allows us to design a WSAN that minimizes QoS while maintaining a particular QoC level.

We apply our approach to a building lighting system in which we control the light level and glare by adjusting artificial lights and venetian blinds. In contrast to traditional (and relatively inefficient) local feedback strategies (e.g., P or PI controllers), which are still widely employed for even the most advanced lighting control systems [12], we introduce a more sophisticated control approach that incorporates the impact of network delays and packet-loss within a Model-Predictive Control (MPC) algorithm. MPC [22] is a control algorithm that computes the current control action by solving, at each sampling instant, a finite-horizon open-loop optimal control problem, using the current state of the plant as the initial state. The optimization process generates an optimal control sequence, the first control value of which is applied to the plant.

Our contributions are as follows:

- We formulate a building lighting control system as an optimal control problem where we minimize network delay and battery energy while maintaining fixed QoC levels (measured in terms of lighting energy usage and user discomfort).
- We empirically study how WSAN QoS affects our QoC metric.
- We compare our proposed algorithm with two baseline controllers (PI and MPC) that use a presence-based strategy, and show that it improves user comfort by an average of 65% for the PI baseline, while decreasing energy usage by 19% and 25% for the PI and MPC baselines, respectively. Furthermore, our algorithm shows a 68% improvement for the QoS compared to the PI baseline networks.

A. Mady and G. Provan are with Cork Complex Systems Lab (CCSL), Department of Computer Science, University College Cork (UCC), Cork, Ireland `mae1,gprovan@cs.ucc.ie`

II. RELATED WORK

There is clear empirical evidence that automated blinds can reduce energy usage, e.g., [14], [18]. However, [9] reports that integrated blinding/lighting systems have not been successful to date, and that the most successful systems use customized control algorithms rather than simple PI controls [14], i.e., the controller must be able to compute optimal combinations of blind tilt/position and indoor light illumination simultaneously. Mukherjee et al. [18] showed that integrating lighting/blinding controls saved 66% over a benchmark of fixed lighting, and 23% over independent control of lighting and blinding. We extend the work of [18] by optimizing user comfort in addition to saving energy, rather than focusing just on energy savings.

In the context of the impact of daylight glare on luminance control, [2] provided a numerical simulation for the blind transmittance based on the glare angle and blind tilt angles, from which we have adopted the same blind transmittance model. [2] augments the daylight coming to the controlled zone using a dimming controller for electric lights, in order to maintain the required luminance. On the other hand, [11] has reported that the occupants often dislike automatic blind control, and has developed manual control models for window blinds that can be a basis for the development of future automated systems. These prior works control blinds in order to provide indoor luminance and visual privacy. However, our design extends venetian-blind control to minimize the impact of reflected glare on user comfort.

BMSs typically incorporate simple control mechanisms in practical applications [6], [13]. We study the use of MPC in such applications. There have been a few approaches that have used MPC for building systems, such as [5], [17], [20]. The novelty of our approach in comparison to this prior work is that we incorporate network QoS within the control loop, whereas prior work assumes fixed deterministic sensor/actuator feedback loops.

There is growing interest in the co-design of networked control systems, e.g., [3], [4]. One of the major focuses of recent work has been the study of scheduling at the network or MAC layer [3], [8], [19]. Other work [16] has put in methods for coping with delays in NCSs using PI control. In contrast to the prior work on NCS co-design, we use MPC rather than PI controls.

III. APPLICATION DOMAIN

We design a lighting controller within buildings with the objective of enhancing user comfort and reducing energy consumption. We achieve this by controlling (a) luminance levels of artificial lights, and (b) reflected glare angle α (using a motorized blind to control the blind angle β), as shown in Fig. 1.

A. Design Specification

We assume that we have sensors to measure luminance level (in Lux) in the middle of the controlled zone, in addition to sensors to measure the incident glare angle γ (in arc-degree) from outside.
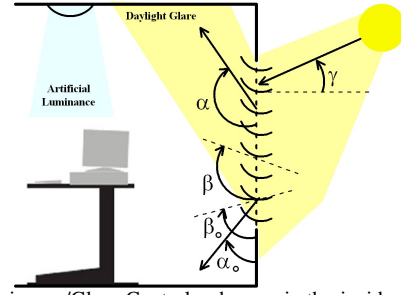

Fig. 1. Luminance/Glare Control, where γ is the incident glare angle, α is the reflected glare angle, α_o is the farthest reflected glare angle from the occupant vision, β is the blind tilt angle and β_o is the optimal blind tilt angle that provides maximum blind transmittance.

In order to demonstrate our control approach, we have modelled a single room that contains two main groups of components, as shown in Fig. 2: (a) environment components reflect the plant physics (e.g., daylight, window blind); (b) control components house the control/sensing algorithm that modify/monitor the environment. Hybrid Systems (HS) [10] are used to create our model, where both discrete (e.g., presence detection) and continuous (e.g., luminance) dynamics are represented. In this context, Linear Hybrid Automata (LHA) are used to describe our HS, where the continuous dynamics are represented using differential/algebraic equations.
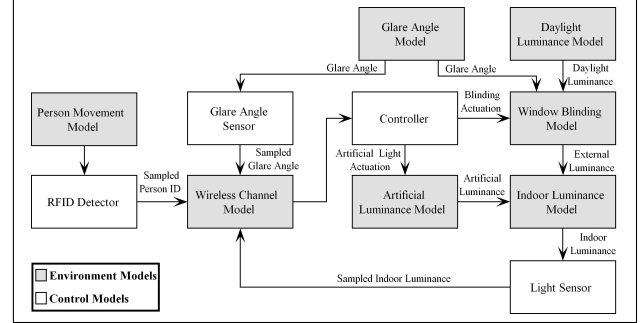

Fig. 2. Environment/Control Model

The main independent variables considered for single-zone control are: (a) the packet-loss probability for the wireless channel; and (b) the sampling period for the sensor (glare angle, light, presence). These variables affect both control and WSAN performance. The environment and control models used for co-design are as follows:

1) Environment Models: Seven environment components have been used; daylight, glare angle, window blind, artificial luminance, indoor luminance, person movement and wireless channel model. We define these as follows:

- *Daylight Model*: The daylight luminance L_d is modelled as a linear differential equation that has five different slopes based on the time of day; during the first and last four hours of the day, the luminance is equal to zero; the differential equation has positive slope during the second four hours; in the next eight hours the slope is equal to zero and then has a negative slope in the following four hours in order to reach zero luminance again at the end of the day.
- *Glare Angle Model*: Our model captures the impact of shifting cloud cover, which randomly changes the glare angle. Hence, we model glare angle γ using a

random variable in the range [15°,65°], triggered for a specific daytime period (i.e. 10am-2pm) and sampled every hour. The variation range of glare angle is based on a real world data set, as described in [2].

- *Window Blind Model*: The blinding model is responsible for identifying the window transmittance τ for the daylight intensity [2] and the reflected glare angle, as depicted in Fig. 1. In this context, two modes are used to calculate the luminance transmittance, where Eq. 1 is used if glare is detected in order to give maximum transmittance at $80°$, while Eq. 2 is used if no glare is present, where maximum transmittance τ_{ng} is given at $90°$. Finally, as in Eq. 3, the external luminance L_{out} that comes from daylight is calculated as a proportion of the daylight luminance L_d based on the window transmittance τ.

$$\tau(\beta,\gamma) = 0.55.e^{\frac{-(\beta-80)^2}{1900}}.(-4.917.10^{-7}.\gamma^4$$
$$+0.00009.\gamma^3 - 0.00567.\gamma^2$$
$$+0.13.\gamma - 0.00437) \tag{1}$$

$$\tau(\beta) = \frac{\tau_{ng}.\beta}{90} \quad (2) \qquad L_{out} = \tau.L_d \quad (3)$$

- *Artificial Luminance Model*: We compute the artificial light (e.g. bulb) intensity L_a in Lux based on the actuation value u_a. In our model we consider the actuator as a luminance dimmer that is linearly proportional to the product of the actuation value and maximum luminance L_a^{max} (i.e., 700 Lux).

$$L_a = L_a^{max}.u_a \tag{4}$$

- *Indoor Luminance Model*: This component provides the total luminance of the controlled zone, and incorporates external luminance, artificial luminance and the luminance interference from the adjacent zones L_a^{adj} (in case of multiple zones), based on the distance r between the adjacent artificial light source and the light sensor, as in Eq. 5.

$$L_{in} = L_{out} + L_a + \frac{L_a^{adj}}{r^2} \tag{5}$$

- *Person Movement Model*: A Markov chain has been used to predict each user's movement in the controller zone (assumed that 3 persons occupy each zone). Three transition matrices P are identified to reflect the user behaviour during the working hours, as in Eq. 6, Eq. 7 and Eq. 8. For example, P_{8-12} is the transition matrix used in the period 8-12 in the morning, where the user movement is predicted each hour.

$$P_{8-12} = \begin{array}{c} \\ in \\ out \end{array} \overset{\overbrace{\begin{array}{cc} in & out \end{array}}}{\begin{bmatrix} 0.9 & 0.1 \\ 0.95 & 0.05 \end{bmatrix}} \tag{6}$$

$$P_{12-14} = \begin{array}{c} \\ in \\ out \end{array} \overset{\overbrace{\begin{array}{cc} in & out \end{array}}}{\begin{bmatrix} 0.5 & 0.5 \\ 0.5 & 0.5 \end{bmatrix}} \tag{7}$$

$$P_{14-17} = \begin{array}{c} \\ in \\ out \end{array} \overset{\overbrace{\begin{array}{cc} in & out \end{array}}}{\begin{bmatrix} 0.1 & 0.9 \\ 0.05 & 0.95 \end{bmatrix}} \tag{8}$$

- *Wireless Channel Model*: In this model, we assumed that the wireless channel has no delay and noise, since these factors have a minor effect on our QoS metric. The channel packet-loss is modelled as a random process whose parameters are related to the behaviour of the network [21]. The measurement at the controller side is given by:

$$\hat{v}(k) = \begin{cases} v(k), & \gamma(k) = 1 \\ v(k-1) & \gamma(k) = 0, \end{cases} \tag{9}$$

where $v(k)$ is the sample value sent from a sensor, $\hat{v}(k)$ is the received sample value at the controller, $\gamma(k)$ is a Bernoulli random variable with $Pr(\gamma(k) = 1) = 1 - p$, and p is the packet-loss probability in the wireless channel model.

2) Control Model: A light sensor, glare angle sensor, Radio Frequency Identification (RFID) detector and controller models are used to monitor and control the environment model. The light sensor samples the indoor luminance once per sample period, and sends the sampled value to the controller. Similarly, the glare angle sensor and the RFID detector are used to sample the glare angle and the person movement, respectively. For the RFID, we use an event-based process that is activated whenever an occupant is detected in the controlled zone.

IV. CO-DESIGN PROCESS

In modern buildings, controllers embedded in large wireless/wired sensor/actuator networks may have their control performance compromised by WSAN delays and lost data. Control theory requires accurate, timely and lossless feedback data; however, random delays and packet-loss are generally accepted in communication networks, particularly in wireless networks. Therefore, the performance of the control model relies on the network performance, due to the distribution and communication-based control. From the control perspective, the more knowledge the controller has about the system, the better the controller can be designed to tolerate communications problems. Additional knowledge about the system can be obtained by increasing the number of sensors or sending sensor measurements more frequently. However, this increases the communication burden on the network, leading to network congestion. The congestion results in longer delays and more packet-losses, which degrade the control performance. The fact that control systems and communication networks are typically designed using different platforms and principles means that co-design is necessary to optimize performance of both systems.

This section defines the overall co-design problem that we are solving, and then outlines the components of this problem. We define in Section IV-A the co-design objective function, and we then define in Section IV-B and Section IV-C the QoS and QoC evaluation, respectively.

A. Co-Design Objective Function

Our co-design methodology considers the correlated parameters between the control application and the other WSAN layers (e.g. MAC, link), which mutually affect both

WSAN QoS and the control performance QoC. In this context, we have selected three parameters that affect both control and WSAN performance: the sampling period h for the light sensor, glare angle sensor and RFID detector (assuming all the sensors use the same h), channel packet-loss probability p and the controlled zone status z (single or multiple).

Our co-design objective function J is decomposed into two sub-functions $J = (J_{QoS}, J_{QoC})$, where J_{QoS} optimises the WSAN performance and J_{QoC} optimises the control performance, as follows:

$$J = (J_{QoS}, J_{QoC})$$
$$= \min_{h} \quad J_{QoS}(h, p, z) \quad s.t. \quad J_{QoC}(h, p, z) \leq J_{req},$$

where

- h is the decision variable,
- J_{QoC} is the quality of control objective function, given by $J_{QoC} = DI + E$, where DI is the discomfort indicator and E is the energy consumption, J_{req} is the upper bound on control quality. In order to avoid having an infeasible solution, J_{req} should be greater or equal than the minimum of the empirical result for J_{QoC}, i.e., $J_{req} \geq min(J_{QoC})$; and
- J_{QoS} is the quality of service objective function, given by $J_{QoS} = d + e_{battery}$, where d is the network delay, i.e., the average time between sending a sample and receiving an actuation, $e_{battery}$ is the energy use for the sensor battery.

In the context of controlling the blind and the indoor luminance, the control objective function is decomposed such that $J_{QoC} = (J_b, J_l)$, where J_b optimizes the blind setting and J_l optimizes the indoor luminance, as will be explained later.

Our co-design methodology considers two optimization stages: (a) the first stage empirically evaluates J_{QoC} over the search space of the decision variables h in order to identify the acceptable range of h that gives $J_{QoC} \leq J_{req}$; (b) the second stage optimizes J_{QoS} conditionally on J_{QoC} in order to empirically evaluate the values of h (among the identified range from the first stage) that minimizes J_{QoS}.

B. WSAN and QoS Evaluation

We assume that we have a WSAN consisting of a set of n wireless nodes, all of which send data to and receive data from a single base station node. Therefore, the average delay over the WSAN is calculated as:

$$d = \sum_{k=1}^{N} \frac{t_r(k) - t_s(k)}{N},$$

where $t_s(k)$ is the time of sending a sample, $t_r(k)$ is the time for receiving the response at the actuator, and N is the total number of samples. In case of missing a sample, the delay time for this sample is calculated as the sampling period for the corresponding wireless node. The battery energy use $e_{battery}$ is evaluated as a linear proportion of the sampling frequency $(1/h)$, where more samples lead to more battery energy use $e_{battery}$.

In order to evaluate each term of J_{QoS} in an equivalent manner (avoiding the dominance from any of the terms), each of $e_{battery}$ and d have been normalized.

1) Network Structure: Fig. 3 presents the wireless network topology, where the actuators are hooked up to the wired network. Each controlled zone contains one light sensor "S", one glare angle sensor "G" (in case the zone includes a window), one actuator "A", three RFIDs "R" and one local controller "C".
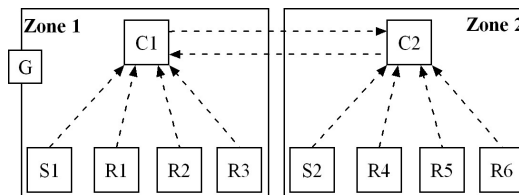

Fig. 3. Network Topology, where C is local controller, G is glare angle sensor, S is light sensor and R is RFID detector.

2) WSN Layered Structure: In our model, we considered three layers of the international standard of an Open System Interconnection (OSI): application, Medium Access Control (MAC), and network layer. The application layer handles the control algorithm, while the MAC layer provides the addressing and channel access control mechanism that enables several network nodes to communicate. Through studying our network structure, we can conclude that the network layer does not have a significant role, given that point-to-point (single-hop) routing is used, i.e., either S/G/R-to-C or C-to-C.

3) MAC Protocol: In our model, a Time Division Multiple Access (TDMA-base) MAC protocol [15] is used in the contention-free period, which leads to a free collision probability. In this protocol, new sensor measurements are generated at the beginning of each sample period, and old packets are dropped when new packets are generated. A packet is declared *lost* if it has not been received by the end of the sample period. TDMA is a collision-free protocol in which time slots are assigned in advance and never changed. We consider fixed TDMA, and assume that time slots are divided evenly among all the transmitter/receiver pairs. Since the time slots are pre-assigned, a time slot can be wasted if the pre-assigned transmitter no longer has a packet to send.

4) Modelling Aspects: In order to model the MAC protocol, two issues have to be considered:

- For modelling the TDMA protocol, we implement a timer for each network node (controller, sensor, RFID) and assign the transmitting time to it. We assume that the node is ideal (no process) until the transmission time is reached.
- We have identified the time slot (the transmission period for the data packet) based on the IEEE 802.15.4 physical layer [23]. In this case, the transmitting data rate is 20 Kbps and the packet length is almost 25 bytes. Therefore, the time slot is equal to ~15ms. For modelling the time slot, we have added the transmission period to the TDMA timer (mentioned in the previous point).

5) Network Assumptions: Our assumptions about network transmission are as follows:

1) Wireless channel delay and transmitting/receiving time are negligible.
2) A packet is declared *lost* if it has not been received by the end of the sample period.
3) The controller commands are always successfully received by the actuator.
4) The sensing and actuation execution time is negligible.

C. Lighting Application Domain and QoC Evaluation

$J_{QoC} = DI + E$, where DI is the discomfort indicator and E is the energy consumption.

- $DI = \sum_{k=k_s}^{k_f} \frac{(y(k) - r(k))^2}{N_{p_z}} p_z(k) +$

  $\sum_{k=k_s}^{k_f} \frac{(\alpha(k) - \alpha_o)^2}{N_{p_z}} p_z(k)$, where the first term considers luminance discomfort measured using the Mean Square Error (MSE) between the indoor luminance $y(k)$ (k varies from k_s to k_f) and the luminance set-point $r(k)$, but only during the occupation periods identified by presence detection variable $p_z(k)$ (equals to 1 in case of presence detection, 0 otherwise) and N_{p_z} is the number of samples for $p_z(k) = 1$. The second term calculates the glare discomfort using MSE between the reflected glare angle $\alpha(k)$ and the farthest glare angle, α_o, from the occupant's vision (which provides the maximum glare visual comfort). In our model, we have selected $\alpha_o = 0^o$, in which case we can guarantee an acceptable level of visual privacy as well.

- $E = \sum_{k=k_s}^{k_f} u_a(k)hP$, where $u_a(k)$ is the actuation value (the dimming percentage) at the kth sample, h is the sampling period and P is the maximum power.

Similar to J_{QoS} evaluation, the J_{QoC} terms are normalized.

V. CONTROL ALGORITHM

As explained earlier, our co-design methodology aims to evaluate the decision variable (i.e., the sensor sampling period h) that optimizes both J_{QoS} and J_{QoC}. We will show that DI and d are monotonic functions of h, but E and $e_{battery}$ are inverse monotonic functions of h. Therefore, the control objective function J_{QoC} is identified to minimize DI and E at each sampling time k.

In this section we formulate an Integrated Model Predictive Controller (IMPC) that decomposes the objective function J_{QoC} into (J_b, J_l), where J_b and J_l are used to optimize the blinding actuation and the artificial luminance, respectively. Since controlling the blind can provide a luminance source with no energy cost, we execute J_b with a high priority. IMPC is considered as a case-study for our co-design methodology, in order to show its QoC and QoS efficiency, as will be explained later.

A. Window Blind Control

The J_b aims to get the maximum luminance from the daylight while reducing the discomfort caused by glare, as in Eq. 10. The first term of J_b improves DI as it minimizes the glare discomfort, and the second term improves E as it leads to less artificial luminance needed to reach the set point:

$$J_b = (\alpha(k) - \alpha_o)^2 + (\beta(k) - \beta_o)^2, \quad (10)$$

where α_o is the user preference for reflected glare angle ($\alpha_o = 0^o$) and β_o is the blind actuation angle that provides the maximum external luminance (the luminance influenced from the daylight). In case of glare detection, the maximum blind transmittance in our model (as described in [2]) is detected at $\beta_o = 80^o$. However in case of no glare, it is detected at $\beta_o = 90^o$, where there is no reflected glare.

The glare plant equation is thus given by:

$$\alpha(k) = \gamma(k) + 2\beta(k) - 90.$$

We minimize J_b by setting the first derivative $\frac{\delta J_b}{\delta \beta}$ to 0, to produce Eq. 11, from which we can calculate β based on γ. In this context, the glare angle variation $\gamma \in [15^o, 65^o]$ leads to variation of $\beta \in [0^o, 180^o]$.

$$\beta(k) = 0.2\beta_o - 0.4(\gamma(k) - \alpha_o - 90). \quad (11)$$

B. Artificial Light Control

The J_l objective function considers DI by minimizing the difference between the indoor luminance $y(k)$ and the reference signal $r(k)$, while minimizing E, using the power consumed by the artificial light. $r(k)$ is calculated as the average of the preferences for the detected persons (using RFID detectors).

MPC is used in this control stage, in order to predict $Y = [y(k+1|k) \dots y(k+N_p|k)]^T$ within a prediction horizon N_p, where $y(k + 1|k)$ is the indoor sensed luminance at $(k + 1)^{st}$ sample given the kth sample. Then, the predictive control system J_l minimizes the energy consumption and tries to reach the reference signal R_s, where we assume that the reference signal remains constant in the optimization window, as in Eq 12. Thus, the objective is to find the "best" actuation vector (in Lux) $\Delta U = [\Delta u(k) \dots \Delta u(k+N_c-1)]^T$ such that we minimize J_l.

$$R_s^T = \overbrace{[11 \dots 1]}^{N_p} r(k) \quad (12)$$

The cost function J_l (solved only when $p_z(k) = 1$) reflects the control objective described in Eq. 13, where the first term is linked to the objective of minimizing the errors between the predicted output and the reference signal. The second term reflects the power used at each sample time starting from $(k + 1)$ to $(k + N_c)$, where N_c is the control horizon. Finally, the last term considers the size of ΔU. $\overline{R}$ is a diagonal matrix with the form $\overline{R} = r_w I$, wehre I is a $N_c \times N_c$ identity matrix, and r_w is used as a tuning parameter for the desired closed-loop performance.

$$\begin{aligned} J_l = {} & (R_s - Y)^T (R_s - Y) \\ & + (u(k) + \Delta U)^T (u(k) + \Delta U) \\ & + \overline{R}\Delta U^T \Delta U \end{aligned} \quad (13)$$

Varying N_p identifies the system sensitivity: ΔU is relatively insensitive to long N_p, but more sensitive (i.e., changes faster to reach the set-point) for short N_p. Since the light system requires fast control, we have selected $N_p = 2$ to enable sufficiently fast lighting-system reactions.

The system model for the lighting process can be described by a linear model, represented in a discrete state space as in Eq. 14 and Eq. 15:

$$x_m(k+1) = A_m x_m(k) + B_m u(k) + C_m w(k) \quad (14)$$

$$y(k) = D_m x_m(k), \quad (15)$$

where $u \in \mathbb{R}$ is the actuation variable (artificial light luminance); $w \in \mathbb{R}$ is the adjacent actuation value (neighbour artificial light luminance); $y \in \mathbb{R}$ is the process output (sampled indoor luminance); and $x_m \in \mathbb{R}^{n \times 1}$ is the state variable.

In order to have a scalable solution for multiple-zone control, we have introduced w in order to capture the adjacent zone actuation. Therefore, our algorithm can predict the interference luminance coming from the adjacent zones using Eq. 5.

Due to the principle of receding-horizon control, where current information of the plant is required for prediction and control, we have assumed that the input $u(k)$ cannot affect the output $y(k)$ at the same time.

We denote the difference of the state variable by $\Delta x_m(k+1) = x_m(k+1) - x_m(k)$, the difference of the actuation variable by $\Delta u(k) = u(k) - u(k-1)$ and the difference of the adjacent actuation value by $\Delta w(k) = w(k) - w(k-1)$. Based on this notation, we see that:

$$\overbrace{\begin{bmatrix} \Delta x_m(k+1) \\ y(k+1) \end{bmatrix}}^{x(k+1)} = \overbrace{\begin{bmatrix} A_m & o_m^T \\ D_m A_m & 1 \end{bmatrix}}^{A} \overbrace{\begin{bmatrix} \Delta x_m(k) \\ y(k) \end{bmatrix}}^{x(k)}$$

$$+ \overbrace{\begin{bmatrix} B_m \\ D_m B_m \end{bmatrix}}^{B} \Delta u(k) + \overbrace{\begin{bmatrix} C_m \\ D_m C_m \end{bmatrix}}^{C} \Delta w(k)$$

$$y(k) = \underbrace{\overbrace{\begin{bmatrix} o_m & 1 \end{bmatrix}}^{D}}_{n} \begin{bmatrix} \Delta x_m(k) \\ y(k) \end{bmatrix} \quad (16)$$

where $o_m = \overbrace{[00\ldots0]}$ and (A, B, C, D) is called the augmented model.

Therefore, a compact matrix form can be concluded from Eq. 16 as:

$$Y = Fx(k) + \Phi \Delta U + \Psi \Delta W; \quad F = \begin{bmatrix} DA \\ DA^2 \\ \vdots \\ DA^{N_p} \end{bmatrix},$$

$$\Phi = \begin{bmatrix} DB & 0 & 0 & \cdots & 0 \\ DAB & DB & 0 & \cdots & 0 \\ \vdots & \vdots & \vdots & \ddots & \vdots \\ DA^{N_p-1}B & DA^{N_p-2}B & DA^{N_p-3}B & \cdots & DA^{N_p-N_c}B \end{bmatrix}$$

$$\Psi = \begin{bmatrix} DC & 0 & 0 & \cdots & 0 \\ DAC & DC & 0 & \cdots & 0 \\ \vdots & \vdots & \vdots & \ddots & \vdots \\ DA^{N_p-1}C & DA^{N_p-2}C & DA^{N_p-3}C & \cdots & DA^{N_p-N_c}C \end{bmatrix}$$

In order to evaluate the optimal ΔU that minimizes J_l, we express J_l as in Eq. 17:

$$J_l = (R_s - Fx(k) + \Psi \Delta W)^T (R_s - Fx(k) + \Psi \Delta W)$$
$$+ u^2(k) - 2\Delta U^T (\Phi^T (R_s - Fx(k) + \Psi \Delta W)$$
$$- u(k)) + \Delta U^T \Delta U (\Phi^T \Phi + \overline{R} + 1) \quad (17)$$

We have used quadratic programming to optimize the objective function J_l, constraining ΔU to the interval $\Delta U \in [\Delta U^{max}, \Delta U^{min}]$, where ΔU^{max} and ΔU^{min} are the maximum and minimum ΔU variation, respectively.

In order to evaluate the computational complexity of our developed distributed control versus centralized, [7] has studied a similar control algorithm and showed that: the computational complexity is $\mathcal{O}(n^3)$ for the centralized controller, whereas our algorithm is $\mathcal{O}(n)$. Moreover, the sensor cost for the centralized network is significantly higher than the distributed algorithm, as the receiver sensor node needs high computational/memory resources in order to support the centralized computational complexity.

VI. EXPERIMENTAL DESIGN

In our experiments, we vary the correlated parameters between the control application and the other WSAN layers (e.g. MAC, link) such as sensor sampling period and channel packet-loss (h, p), which mutually affect both J_{QoS} and J_{QoC}. For example, if we have an input 2-tuple $(5min, 3\%)$, we will measure outputs $J_{QoC} = 0.97$ and $J_{QoS} = 0.39$.

This section describes the experimental design used to study (done through simulation) the relevant parameters in our co-design process.

A. Baseline Specification

In order to evaluate the efficiency of our developed control algorithm (IMPC), we have used standard PI and MPC control algorithms as a baseline control model. In this model, one light sensor is used to detect the indoor luminance and one Passive InfraRed (PIR) sensor detects the user motion. The controller set point is fixed to 500 Lux (optimal luminance at European law UNI EN 12464) whenever a person is detected in the controlled zone. In this case, the blind is controlled manually, where the user avoids glare by shutting the blind whenever glare is detected.

B. Dependent/Independent Variable

In our experimental design, we consider three independent variables as follows:

- Sensor sampling period h: considers the sampling period for light sensor, glare angle sensor and RFID detector. The search space is $h \in \{1, 5, 10, \ldots, 30\}[minutes]$.
- Channel packet-loss probability p: has search space $p \in \{1, 2, \ldots, 5\}[\%]$.
- Controlled zone status (i.e. single (S) or multiple (M)): $z \in \{S, M\}$.[1]

The dependent variables J_{QoC}, J_{QoS} are evaluated for each experiment in the search space of the independent-variable cross product $h \times p \times z$. Considering the probabilistic components in our model, we run each experiment several times and then average the resulting outputs over p.

---

[1] In this article, we consider only a single controlled zone, i.e. $z = S$.

C. Empirical Results

As explained in Section IV-A, firstly we consider the control performance J_{QoC} in order to identify the values of the decision variable h that give acceptable performance. The control performance J_{QoC} evaluates two matrices: (a) energy consumption E as shown in Fig. 4; and (b) user discomfort indicator DI, which considers luminance discomfort as in Fig. 5 and glare discomfort as in Fig. 6.

Fig. 5 and Fig. 6 show that DI increases when h increases, because the controller needs time proportional to h to tune its decision, which leads to hampering the user. Fig. 5 shows improvement in the visual luminance comfort for IMPC compared to the PI baseline. However, the MPC baseline shows better visual luminance comfort than IMPC, as controlling the daylight luminance in IMPC slightly hampers the user.

Fig. 4 and Fig. 5 show the trade-off between the energy consumption and luminance discomfort. The energy consumption for the PI baseline decreases when h increases; in contrast, for the MPC and IMPC algorithms energy use is "almost" constant. Furthermore, IMPC shows the most efficient energy use in comparison to the MPC and PI baselines.

Fig. 7 summarizes our J_{QoC} results. In our analysis, we have normalized each term of J_{QoC}, given a maximum value of J_{QoC} of 3. Assuming $J_{req} = 1.5$, the decision-variable values that satisfy $J_{QoC} \leq J_{req}$, in case of our developed controller, are $h \in \{1, 5, 10\}$. However, in case of a PI controller $h = 1$ and for MPC $h \in \{1, 5, 10, ..., 30\}$.

The WSAN performance, denoted by J_{QoS}, is governed by the network delay d and battery energy $e_{battery}$ terms. d increases when h increases, as in Fig. 8, and $e_{battery}$ increases when $1/h$ increases (sensor sampling rate). Fig. 8 shows "almost" the same d for the baseline and the IMPC network topology, as d evaluates the average delay value. However the developed topology has a higher absolute network delay, because it contains more sensors than the baseline topology.

J_{QoS} is calculated as the sum of normalized d and $e_{battery}$ terms, as shown in Fig. 9. At this stage, we can identify the value of h that satisfies the J_{QoC} limit and minimizes J_{QoS}. $h = 5$ is the optimal value in our developed algorithm and in the MPC baseline. The PI baseline controller has only one choice (from the control performance evaluation stage), i.e., $h = 1$.

Our developed controller shows 19% and 25% average energy consumption saving (over all the experiments) compared to the PI and MPC baselines, respectively, and 63% average improvement in the user comfort over the PI baseline. Moreover, it shows 68% QoS improvement over the PI baseline. The use of a higher value of h is the main source of the QoS improvement for IMPC over the PI baseline.

On the other hand, a TDMA-based MAC protocol shows a drawback in glare detection (Fig. 6) at $h = 25$, where the glare angle change (occurring each hour) is missed at the beginning of the sampling period, and hence it is detected in the next sample (which introduces user dissatisfaction).

Therefore, we will consider in future work a dynamic sampling period technique at the MAC protocol.
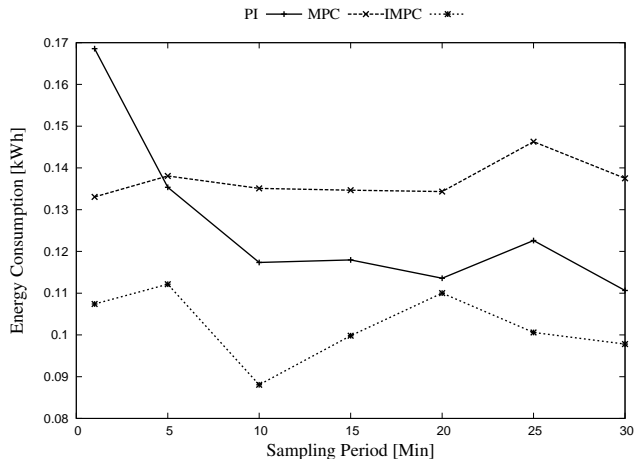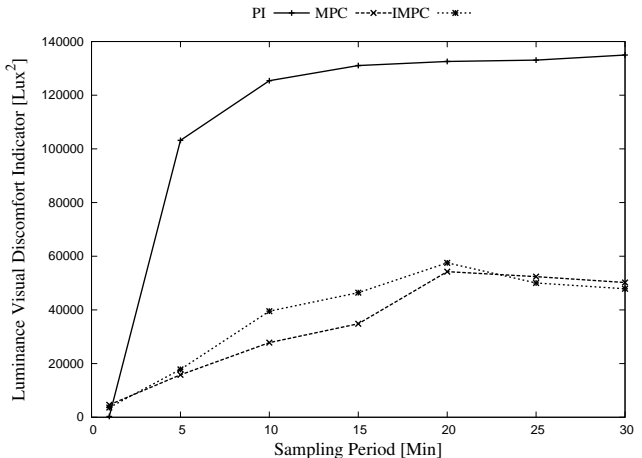

Fig. 4.   Energy Consumption
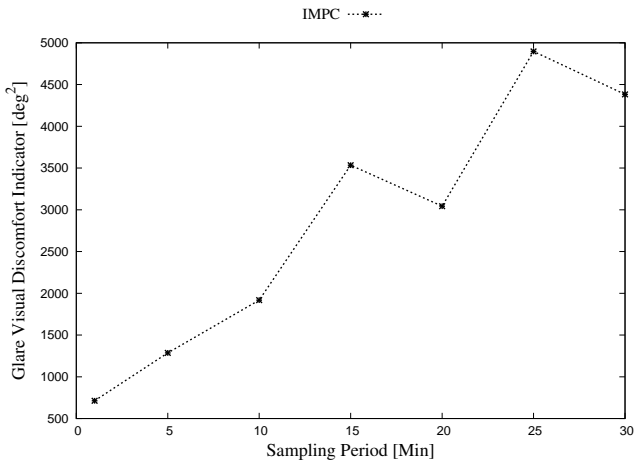

Fig. 5.   Luminance Visual User Discomfort

Fig. 6.   Glare Visual User Discomfort

VII. CONCLUSIONS AND FUTURE WORK

This article introduces a co-design methodology that optimizes the WSAN performance while maintaining the control performance within an acceptable range. We have applied the developed co-design methodology on a novel lighting controller. We compared our proposed algorithm with two state-of-the-art controllers (PI and MPC) that use a presence-based strategy, showing that it improves user comfort by
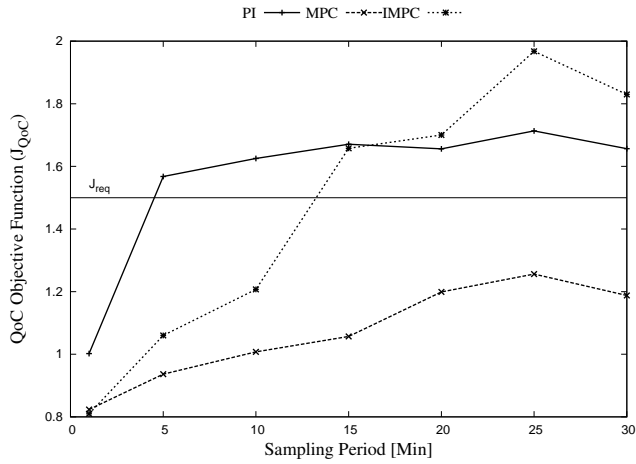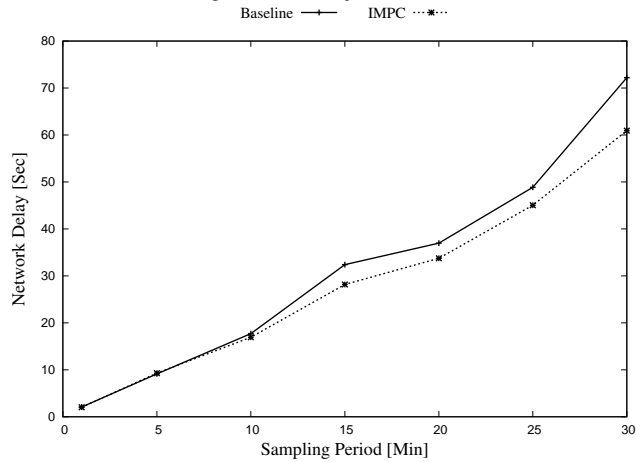
Fig. 7. QoC Objective Function
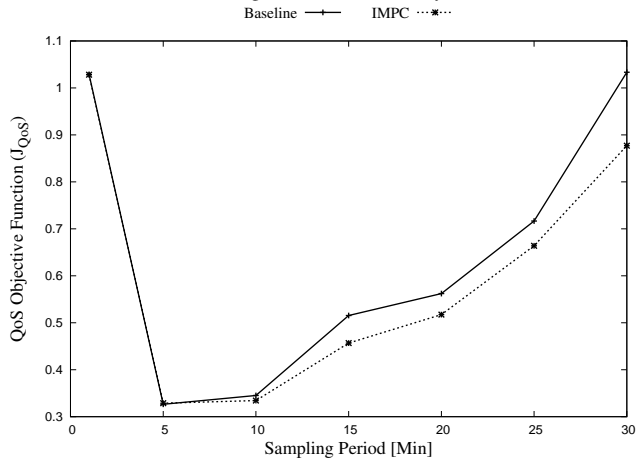

Fig. 8. Network Delay

Fig. 9. QoS Objective Function

an average of 65% over the PI baseline, while decreasing energy usage by 19% and 25% over the PI and MPC baselines, respectively. Furthermore, our algorithm shows a 68% improvement for the QoS in comparison to the PI baseline networks.

In future work, we plan to extend this co-design methodology to consider a distributed control system as well as multi-zone building applications, and to extend our co-design objective function to consider different MAC protocols.

REFERENCES

[1] Scenarios for a clean energy future: Interlaboratory working group on energy-efficient and clean-energy technologies. The Interlaboratory Working Group on Energy-Efficient and Clean-Energy, 2000. NREL/TP-620-29379; ORNL/CON-476; LBNL-44029.

[2] A. K. Athienitis and A. Tzempelikos. A methodology for simulation of daylight room illuminance distribution and light dimming for a room with a controlled shading device. *Solar Energy, Elsevier Science*, 72:271–281, 2002.

[3] C. Aubrun, D. Simon, and Y.Q. Song. *Co-design Approaches to Dependable Networked Control Systems*. Wiley-IEEE Press, 2010.

[4] C. Bo, GAO Xiu-e, and Z. Zhi-wu. Co-design of networked control system based on QoS management. *Journal of Liaoning Technical University*, 1, 2006.

[5] V. Chandan, S. Mishra, and A. Alleyne. Predictive control of complex hydronic systems. *American Control Conference (ACC)*, pages 5112–5117, 2010.

[6] V. Chandan, S. Mishra, and A.G. Alleyne. Predictive control of complex hydronic systems. In *American Control Conference (ACC), 2010*, pages 5112–5117. IEEE, 2010.

[7] J. Chen, X. Cao, P. Cheng, Y. Xiao, and Y. Sun. Distributed Collaborative Control for Industrial Automation With Wireless Sensor and Actuator Networks. *IEEE Transactions on Industrial Electronics*, 57:4219–4230, 2010.

[8] J. Chen and B. Lei. Network scheduling and optimal guaranteed cost control co-design. In *Intelligent Control and Automation (WCICA), 2010 8th World Congress on*, pages 4366–4371. IEEE, 2010.

[9] E. Cunill, R. Serra, and M. Wilson. Using Daylighting Controls in Offices? Post Occupancy Study about their integration with the Electric Lighting. In *PLEA2007 - The 24th Conference on Passive and Low Energy Architecture*, Singapore, 2007.

[10] T.A. Henzinger. The theory of hybrid automata. *Proc. 11th Annual IEEE Symposium on Logic in Computer Science (LICS 96)*, pages 278–292, 1996.

[11] V. Inkarojrit. Developing predictive venetian blinds control models using visual comfort predictors. *The 23rd Conference on Passive and Low Energy Architecture*, 2006.

[12] D. Kolokotsa, A. Pouliezos, G. Stavrakakis, and C. Lazos. Predictive control techniques for energy and indoor environmental quality management in buildings. *Building and Environment*, 2008.

[13] D. Kolokotsa, A. Pouliezos, G. Stavrakakis, and C. Lazos. Predictive control techniques for energy and indoor environmental quality management in buildings. *Building and Environment*, 44(9):1850–1863, 2009.

[14] E.S. Lee and S.E. Selkowitz. The New York Times Headquarters daylighting mockup: Monitored performance of the daylighting control system. *Energy and Buildings*, 38(7):914–929, 2006.

[15] A. Liu, H. Yu, and L. Li. An energy-efficiency and collision-free mac protocol for wireless sensor networks. *61st IEEE Vehicular Technology Conference*, 2005.

[16] E.C. Martins and F.G. Jota. Design of networked control systems with explicit compensation for time-delay variations. *Systems, Man, and Cybernetics, Part C: Applications and Reviews, IEEE Transactions on*, 40(3):308–318, 2010.

[17] P. Morosan, R. Bourdais, D. Dumur, and J. Buisson. A dynamic horizon distributed predictive control approach for temperature regulation in multi-zone buildings. *18th Mediterranean Conference on Control & Automation (MED)*, pages 622–627, 2010.

[18] S. Mukherjee, D. Birru, D. Cavalcanti, E. Shen, and M. Patel. Closed Loop Integrated Lighting and Daylighting Control for Low Energy Buildings. 2010.

[19] Y. Niu, X. Wu, J. Kang, and J. He. Method of control performance and network QoS co-design of networked control systems. In *Control and Decision Conference (CCDC), 2010 Chinese*, pages 108–113. IEEE, 2010.

[20] F. Oldewurtel, A. Parisio, C. Jones, M. Morari, D. Gyalistras, M. Gwerder, V. Stauch, B. Lehmann, and K. Wirth. Energy efficient building climate control using stochastic model predictive control and weather predictions. *American Control Conference (ACC)*, pages 5100–5105, 2010.

[21] P. Park, J. Araujo, and K. H. Johansson. Wireless Networked Control System Co-Design. In *IEEE International Conference on Networking, Sensing and Control (ICNSC)*. IEEE, 2011.

[22] L. Wang. *Model Predictive Control System Design and Implementation Using MATLAB*. PAdvances in Industrial Control, Springer-Verlag London, 2009.

[23] J. Wilson. Sensor technology handbook. *ELSEVIER, ISNB:0-7506,77729-5*, 2005.